Hindawi Publishing Corporation
International Journal of Distributed Sensor Networks
Volume 2012, Article ID 545148, 10 pages
doi:10.1155/2012/545148

Research Article

Multisensors On-Site Monitoring and Characteristic Analysis of UHV Transmission Tower

Hai-Feng Bai,[1] Ting-Hua Yi,[2] Hong-Nan Li,[2] and Liang Ren[2]

[1] *School o f Civil and Safety Engineering, Dalian Jiaotong University, Dalian 116028, China*
[2] *Faculty of Infrastructure Engineering, Dalian University of Technology, Dalian 116023, China*

Correspondence should be addressed to Ting-Hua Yi, yth@dlut.edu.cn

Received 19 June 2012; Revised 23 August 2012; Accepted 25 September 2012

Academic Editor: Gangbing Song

It is important to clarify the variational rules between dynamic characteristics and gust response factors (GRFs) of an ultra high-voltage (UHV) transmission tower for the structural design. In this paper, the synchronous multisensors on-site monitoring has been carried out under field wind conditions, which includes field fluctuating wind velocity, acceleration responses, and base bending strains on parts of the just-built transmission tower. The dynamic characteristics of tested transmission tower were investigated by a modal identification method (MIM) and validated those results with a finite-element method (FEM). Similarly, the GRFs based on the top displacement or base dynamic bending stains are calculated and compared by means of a measurement data statistical method and some different quasistatic methods, respectively. The results have shown that the dynamic characteristics obtained from the measurement data analysis with the MIM agree with those from the FEM, which confirms that the FEM and the MIM for dynamic characteristics are consistent and correct. In turn, the GRFs form the measurement displacement analyses have some differences from those calculated with the quasistatic method, and it is necessary to further identify and verify their causations.

1. Introduction

Transmission tower-line system (TTLS) is a dynamic response-sensitive structure system under wind loading, which is sensitive with analytical model and load uncertainty as well as many unpredictable difficulties in the reliability evaluation of the used structures for designer [1]. Thus, it is important to clarify the variational rules between dynamic characteristics and GRFs of UHV transmission tower for the structural design. The present studies indicate that there are two reasons for this situation. The first one is that once such transmission-line system has been built and put into use, it becomes a bearing high electric energy system. In such situation, it's difficult to monitor its structural responses induced by the environmental load. The second one is that, there is a parameter limitation with a specific structure design process from different specifications or specific monitoring. As for the integrity of such a structure system and its uncertainty, it is very necessary to carry out a comparative study between experimental test analysis and structural design theory for such transmission-tower structures.

As a result of some economic and technical limitation for the on-site testing and monitoring of transmission tower, some pervious methods for its dynamic response analysis and structure design are mostly to choose the numerical analyses or wind tunnel tests [2–4] so that the measurement data and its corresponding analytical results are very limited. Based on the full-scale measurement data, Takeuchi et al. [5] studied aerodynamic damping properties of two towers under strong wind conditions. Meanwhile, they established a new method which was applicable to the response record of a multidegree-of-freedom system such as the coupled structure of transmission tower-and-conductors, resulting in that the wind speed dependency of the aerodynamic damping property of the coupled tower-and-conductors system had wide differing characteristics depending on the vibration mode. Lam and Yin [1] and Yin et al. [6] carried out a feasibility study of utilizing ambient vibration data measured from a limited number of sensors in the structural damage detection of transmission towers. The proposed methodology can identify the damaged substructure by estimating the "equivalent" stiffness reduction even in the presence of

Figure 1: The different measurement states of transmission tower-line system.

both measurement noise and modeling error. Momomura et al. [7] and Okamura et al. [8] took the leader on the field monitoring for the wind characteristics and dynamic responses of transmission tower of an TTLS in a mountainous area and then simulated the mountain area wind field in a wind tunnel. These researches found that the aerodynamic response values of acceleration and strain of the tower with conductors and tensile forces of conductors increased in proportion to the power of wind speed. Harikrishna et al. [9], in order to test the designed structural reliability of a communication tower, carried out a comparative study on the results from the measurement data analysis and the design methods of different specifications, respectively. Savory et al. [10] established a hurricane forcing calculation model and its corresponding failure analytical method for the TTLS damage in a middle latitude area caused by the extreme wind load of tropical storm. Paluch et al. [11] based on the statistical analysis of a transmission-crossing long-term field testing data, obtained the wind field properties and the structural response rules, and then analyzed their consistency with a numerical analytical method. Comparatively, the theoretical analysis combined with the field measurement for the TTLS is rarely developed, and making a fore-step advance in this aspect is very useful.

In this paper, taken a just-built transmission tower of a TTLS in Gaizhou city in Liaoning province, as an investigated object, its dynamic characteristics and structural parameters have been measured and analyzed with both of a with-line and a without-line working conditions. In turn, a method for solving the GRFs which related structural dynamic characteristics has been presented; then the various analytical results of the GRF obtained from the measurement data analytical method and different quasistatic structural design methods are comparatively analyzed. Therefore, multisensors on-site monitoring test, wind-induced vibration analyses, and quasistatic design method have been integrated as a system for solving the design problem of a TTLS.

2. Multisensors On-Site Monitoring Test for Transmission Tower

2.1. Structure Feature of Transmission Tower. A transmission crossing is located in Gaizhou City in Liaoning, which belongs to a part of a just-built 550 kV TTLS. The monitored main tower is a type of SZ21 straight line tower, with total height of 56.9 m (nominal height 33 m), tower base width of 8.84 m and tower top width of 2.0 m. There are three crossing arms, respectively, located on the top, middle, and bottom of the tower up-position, in which its minimum arm length is 8 m. The tower can be divided into two segments with uniform taper section on its nominal height and its section gradually shrinking to upwards. Its two adjacent spans are 426 m and 294 m, respectively. The structural diagram and composites of the transmission tower are shown in Figure 1 and Table 1, respectively.

2.2. Multisensor Monitoring Arrangement. In order to obtain some analytical contrast results from the measurement data, structure dynamic characteristics, and quasistatic design parameters of transmission tower, the field multisensor monitoring on the tower working conditions of with-lines and without-lines have mainly been measured for three transmission tower related terms, that is, the acceleration responses at the representative positions, the dynamic strains of the base leg members, and the wind velocity at the 10 m height recommended by wind load standards. Taking little difference of wind velocity variation within the height of transmission tower and anemometer measurement sensitivity into account, a wind velocity measurement point is arranged on the 10 m height position of tower. The wind velocities on other positions from the base to the top of the tower can calculate its mean values according to wind velocity index profile distribution property, and wherein its turbulence intensity is taken to be 0.145 as a result of its terrain characteristics, so that on different heights of

Table 1: The structural composites of the transmission tower and lines.

Segment	Main members	Secondary members	Remarks
1	Q345-L160 × 14, L100 × 8	Q235-L63 × 5, L50 × 5, L45 × 5	Up-crossing bars
2	Q345-L90 × 7, L100 × 8, L160 × 14	Q235-L63 × 5, L50 × 4, L45 × 4, L40 × 4	Middle crossing bars
3	Q345-L160 × 4, L100 × 8, L80 × 7	Q235-L56 × 5, L50 × 5, L45 × 4, L40 × 3	Bottom-crossing bars
4	Q345-L100 × 8	Q235-L90 × 7, L80 × 6, L63 × 5, L56 × 4, L40 × 3	Top segment of tower
5	Q345-L140 × 10, L100 × 8, L80 × 6	Q235-L90 × 7, L75 × 6, L63 × 5, L50 × 4, L45 × 4, L40 × 3	Middle segment of tower
6	Q345-L160 × 10, L110 × 8	Q235-L75 × 6, L70 × 6, L40 × 3	Middle segment of tower
7	Q345-L160 × 12, L140 × 10, L100 × 8	Q235-L90 × 7, L80 × 7, L70 × 5, L40 × 3, L50 × 4, L40 × 3	Middle segment of tower
8	Q345-L180 × 14, L160 × 10	Q235-L90 × 7, L100 × 8, L80 × 6, L70 × 5, L50 × 4, L45 × 5	Middle segment of tower
9	Q345-L200 × 14, L180 × 12	Q235-L90 × 7, L80 × 6, L56 × 4, L50 × 4	Middle segment of tower
10	Q345-L200 × 14, L180 × 12	Q235-L90 × 7, L90 × 8, L80 × 7, L75 × 6, L56 × 5, L50 × 5, L45 × 4	Middle segment of tower
11	Q345-L90 × 7, L200 × 14, L180 × 14, L160 × 12, L100 × 8	Q235-L90×7, L80 × 6, L75 × 5, L63 × 5, L56 × 4, L50 × 4, L45 × 4, L40 × 3	Bottom leg of tower
12	Conductors	4 × JGJ-400/35	
13	Ground lines	JGJ-95/55	

the tower, the measured wind velocities (or wind loads) are diverse. The acceleration monitoring is used with a telemetry data receiving system (TDR03) of which sampling frequency is set to 50 Hz and provides 8 channels for 8 representative positions of the transmission tower and measures the acceleration data on the windward direction. The dynamic strains of the main leg members are measured by means of an optical fiber strain sensor monitoring system of which sensors are arranged on the side of the 4 main leg members above 2.0 m of the tower foundation.

All accelerometers, strain sensors, and an anemometer are connected to their respective data receiving systems as well as acquiring the data for 10 min at the meantime. The concrete sensor instruments and installation positions of the multisensors monitoring equipments are shown in Figure 2. The anemometer is arranged on the position with approximately 10 m height to the foundation level of transmission tower around which is a terrain of open flat farmland. The typical measurement wind velocity time history at the height 10 m is shown in Figure 3.

Herein, in order to compare the consistency between the measurement statistical results and numerical analytical results from the finite-element model of transmission tower structure, the dynamic characteristic parameters are determined and compared through a parameter identification of response mode, which excited by the measurement loads and analyzed by the FEM, respectively.

The modal identification method (MIM) is a method that derives the structural characteristics from the obtained excitation and responses, in the light of the number of excitation, which can be divided into both approaches of single-point excitation and multiple-point excitation. As the complexity of transmission tower is a high-rise structure with large flexible characteristics and during the monitoring wind loading energy is not large enough, and the MIM is conducted for multiple reference points in frequency domain, that namely, using multiple-point excitations and multiple-point responses of the measurement signals, accurately estimating a frequency response function, the modal parameters are directly identified form the relationship between the frequency response functions and modal parameters. The node displacement values should take the mean values from the nodes of a transmission tower in a high level. The details about this theory and method can be referred to in the literature [12–14]. The excitations for the parameter identification can take the measurement wind velocity time histories, and those of responses correspondingly take the acceleration time histories.

In order to analyze the influence of transmission lines on dynamic characteristics of transmission tower, the single tower model (without-lines tower model) and tower-lines model (with-lines model) have been built. In the former, the main members of transmission tower are simulated by the beam elements, and its secondary support members are substituted by the spatial bar elements. In the latter, the tower-lines structural system is truncated as "three towers and two spans" finite-element model, in which the lines are simulated as cable elements, and the tower members are the same as these of the single tower model. Under the conditions of without-lines and with-lines on tower, the dynamic characteristics of the structure from the MIM and the FEM, respectively, are shown in Tables 2 and 3. Meanwhile, in Figure 4, the first-order vibration modes in both orthogonal directions are presented. From Tables 2 and 3 and Figure 4, it can be seen that the first three-order natural frequencies of the transmission tower in in-plane are comparatively close to those in out-of-plane, and the in-plane nature frequencies are slightly larger than those in out-of-plane, which may be

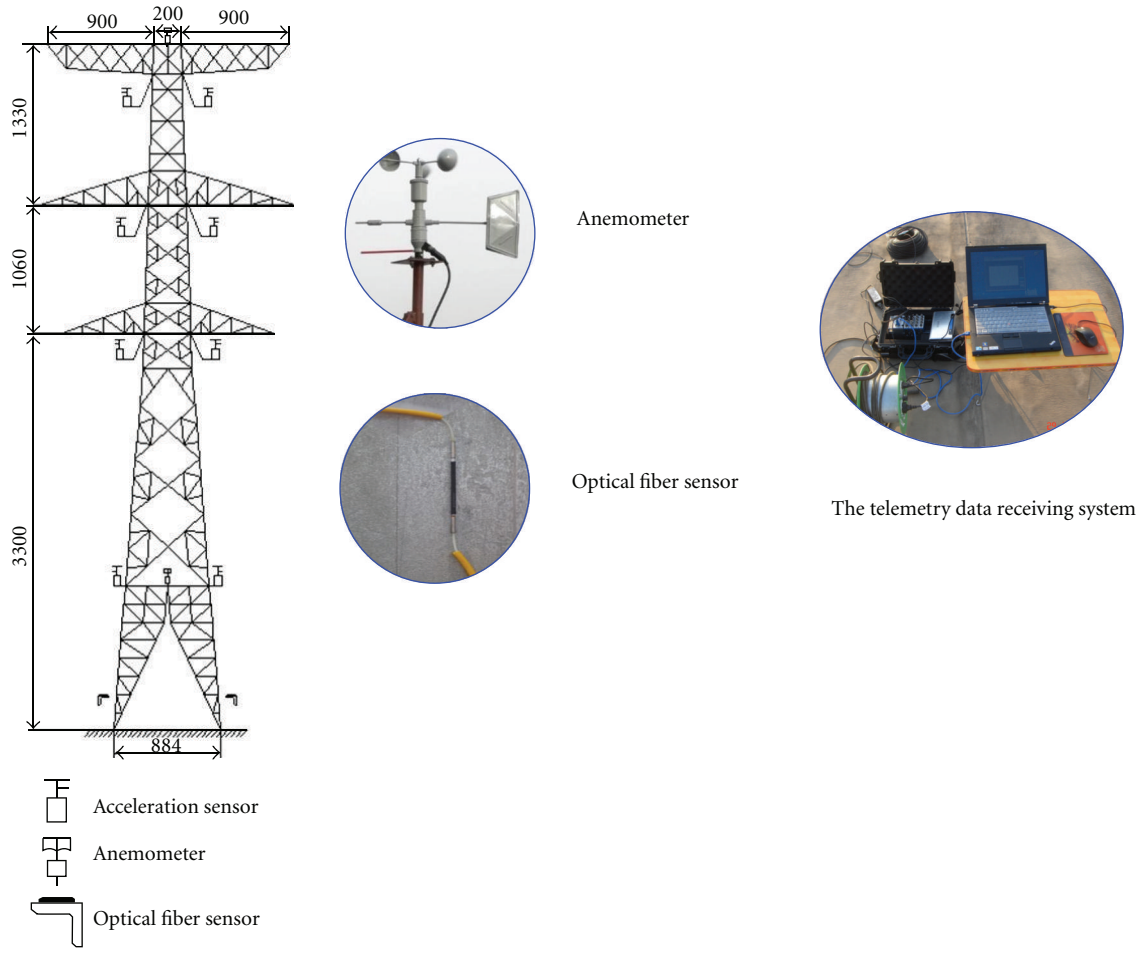

Figure 2: The transmission tower structure and measuring instruments installation.

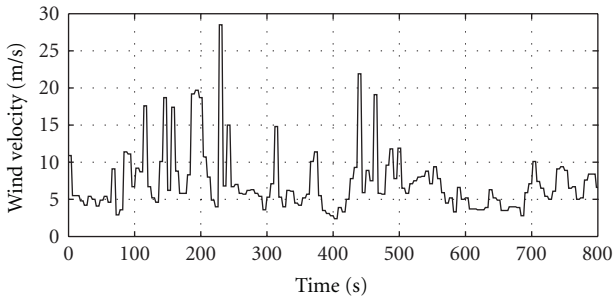

Figure 3: The typical measured wind velocity time history.

associated with the mass differential distribution of cross-arms of tower in two orthogonal directions that indicates the differential damping-mass effect. The results obtained from the FEM are much better in agreement with those of the MIM, the relative deviation between them is about 5%, which indicates that the finite-element numerical model and its results are credible.

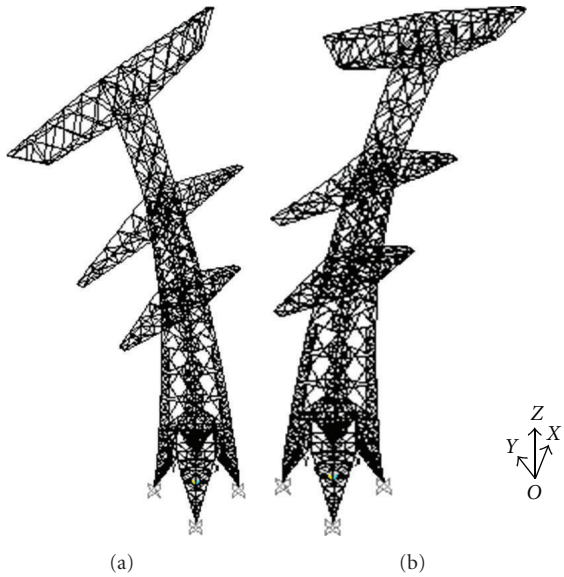

Figure 4: Vibration types of the first mode: (a) out-of-plane; (b) in-plane.

Table 2: The natural frequencies of transmission tower without lines (Hz).

Nature frequency	MIM			FEM		
	The first-order mode	The second-order mode	The third-order mode	The first-order mode	The second-order mode	The third-order mode
XOZ plane (out-of-plane)	1.611	4.847	6.471	1.525	4.660	6.370
YOZ plane (in-plane)	1.622	4.909	6.588	1.554	4.848	6.549

Table 3: The natural frequencies of transmission tower with lines (Hz).

Nature frequency	MIM			FEM		
	The first-order mode	The second-order mode	The third-order mode	The first-order mode	The second-order mode	The third-order mode
XOZ plane (out-of-plane)	1.512	4.568	6.185	1.487	4.479	6.095
YOZ plane (in-plane)	1.544	4.647	6.235	1.503	4.522	6.163

3. Gust Response Factor from Measurement Data

3.1. Gust Response Factor Based on Displacement. Because the displacement sensor for measuring directly the displacement is usually expensive, such as a laser displacement sensor, but the usage of normal displacement sensor needs to set a reference structure, it is very difficult to directly measure the displacement response on various parts of transmission tower. In relative terms, the measurement technology of acceleration time history is relatively mature and practical. Taking into account the acceleration response in combination with the wind velocity time history, the corresponding displacement response curves can be obtained from the quadratic numerical integration of the motion equations as well as the displacement signal filtering out of their lower-frequency components. For this method, the precision can fully meet the dynamic characteristic analysis of transmission tower. The power spectral density curves of the measurement displacement at the tower top are shown in Figure 5, and the GRF of the measurement displacement can be defined by the ratio of the peak value versus mean value of the displacement. As for the mean wind effects from different wind velocity profiles, the relevant tower top displacements can be calculated by the finite-element model established in the second section. In this way, the limitation of the average displacements obtained from the accelerometer data analysis can be overcame. In analysis, it should be paid attention to which theoretically analytical conditions must be consistent with the measured wind velocities and their directions. The GRF based on the displacement can be expressed as follows:

$$G_x = 1 + \frac{g_{ex}\sigma_{ex}}{\bar{x}_t}, \tag{1}$$

where $\bar{x}_t$ is the mean displacement response form the theoretical calculation, σ_{ex} denotes a root mean square (RMS) value of measurement displacement response which is obtained from the integral of acceleration response, and g_{ex} means a statistical peak factor derived from the response process that is assumed as the random Gaussian process, namely,

$$g_{ex} = \sqrt{2\ln(\gamma_{ex}T)} + \frac{0.5772}{\sqrt{2\ln(\gamma_{ex}T)}}, \tag{2}$$

where T denotes an observation duration 600 s and γ_{ex} is an effective zero crossing frequency, that is,

$$\gamma_{ex} = \left[\frac{\int_0^\infty n^2 S_x(n)dn}{\int_0^\infty S_x(n)dn}\right]^{1/2}, \tag{3}$$

where n represents the frequency (Hz) and $S_x(n)$ means a displacement power spectral density function.

Under the wind excitations with different turbulence intensities, the GRF for the displacement calculation obtained from the measurement acceleration integral is shown in Table 4. From the data analysis, it can be concluded that as the increasing of the mean wind velocity and turbulence intensity, the dynamic displacement response at the tower top is strengthened, and the GRF of displacement also increases gradually. The reasons for the phenomena can be attributed to two aspects; on one hand, the increase of turbulence intensity means the RMS deviation of the measurement displacement increased; on the other hand, the displacement mean value increasing can be regarded as the increase of mean wind velocity inducing windward force on the tower enhancing. Thereby, the rules reflected in Table 4 conform to the dynamic response characteristics under the fluctuating wind load.

3.2. GRF Based on Bending Moment. For the reason of field monitoring of transmission tower, it is impossible to control natural wind velocity to zero for balancing a resistor bridge of strain gauge; so only the fluctuating effect of dynamic strains

Table 4: GRF values for top displacement from acceleration measurements.

No.	Mean wind velocity $\overline{V}_{56.9}$ (m/s)	Turbulence intensity	Displacement peak factor g_{ex}	Displacement RMS σ_{ex} (cm)	Theoretical displacement mean values $\overline{x}_t$ (cm)	Displacement GRF
1	8.70	0.06	4.039	0.986	4.887	1.815
2	9.48	0.75	4.046	1.253	5.904	1.858
3	10.36	0.10	4.057	1.584	7.210	1.891
4	11.44	0.11	4.089	2.158	9.021	1.978
5	12.09	0.13	4.120	2.537	10.153	2.029
6	13.21	0.14	4.082	3.216	11.575	2.134
7	14.21	0.16	4.095	3.749	12.637	2.215
8	15.03	0.15	4.110	4.305	13.429	2.318
9	13.65	0.13	4.107	2.934	10.768	2.119
10	11.90	0.11	4.072	2.083	8.952	1.947
11	9.36	0.09	4.065	1.632	6.733	1.985
12	7.45	0.08	4.052	1.038	5.071	1.829
Mean value						2.010

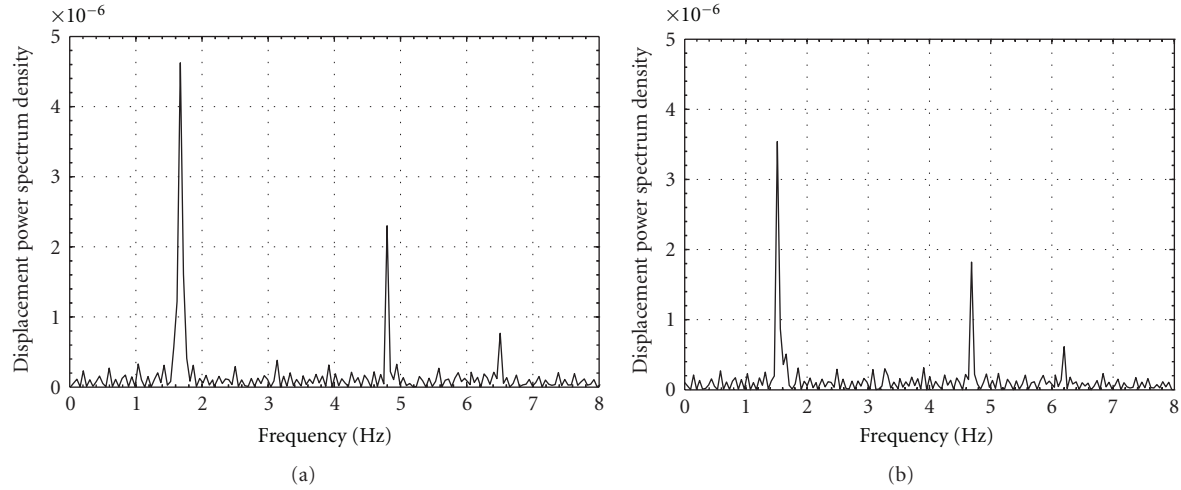

Figure 5: The power spectral density of top displacement: (a) without lines; (b) with lines.

has been taken into account for the measured data analysis. The power spectral density curves of the measurement strains of base-leg members are shown in Figure 6. The GRF based on the bending moment is defined by a ratio of the strain peak value versus its mean value of the main leg members at corresponding measure points. The strain peak factor and its RMS deviation can be obtained from the measurement data analysis under various wind velocities, and the mean strains of measurement points near to the tower foundation of main leg members can be calculated through the FEM from the corresponding wind velocities. As the measurement strains are obtained from the four main legs of transmission tower, those values are invariably different under the conditions of different wind velocities and directions, sometimes, even not in the same magnitude. Thus, the theoretical analysis should be consistent with monitoring conditions. Similarly, the GRF based on the bending moment can be expressed as the following formula:

$$G_\varepsilon = 1 + \frac{g_{e\varepsilon}\sigma_{e\varepsilon}}{\overline{\varepsilon}_t}, \tag{4}$$

where $\overline{\varepsilon}_t$ is the mean strain response from theoretical calculation, $\sigma_{e\varepsilon}$ denotes the RMS value of measurement strain response, and $g_{e\varepsilon}$ means the statistical peak factor derived from the response process that assumed as the random Gaussian process, of which calculation method is the same as formula (2).

Taking into account various factors including wind directions, velocities, and turbulence intensities, the representative measurement strain data of the main legs are selected, and then the GRF based on bending moment is calculated as shown in Table 5. From Table 5, it can be seen that the law of

Table 5: GRF values for base bending moment from strain measurements.

No.	Mean wind velocity $\overline{V}_{56.9}$ (m/s)	Turbulence intensity	Strain peak factors $g_{e\varepsilon}$	Strain RMS $\sigma_{e\varepsilon}$	Theoretical strain mean values $\overline{\varepsilon}_t$	Bending GRF
1	8.70	0.06	3.479	6.16	11.239	2.907
2	9.48	0.75	3.798	6.86	13.611	2.914
3	10.36	0.10	3.771	8.79	15.856	3.091
4	11.44	0.11	3.590	13.72	23.363	3.108
5	12.09	0.13	3.737	14.37	25.795	3.082
6	13.21	0.14	3.651	19.95	32.329	3.253
7	14.21	0.16	3.725	22.45	35.694	3.343
8	15.03	0.15	3.803	23.59	37.127	3.417
9	13.65	0.13	3.698	14.085	26.045	3.000
10	11.90	0.11	3.643	13.88	23.761	3.128
11	9.36	0.09	3.821	7.38	14.134	2.995
12	7.45	0.08	3.577	6.59	12.253	2.923
Mean value						3.097

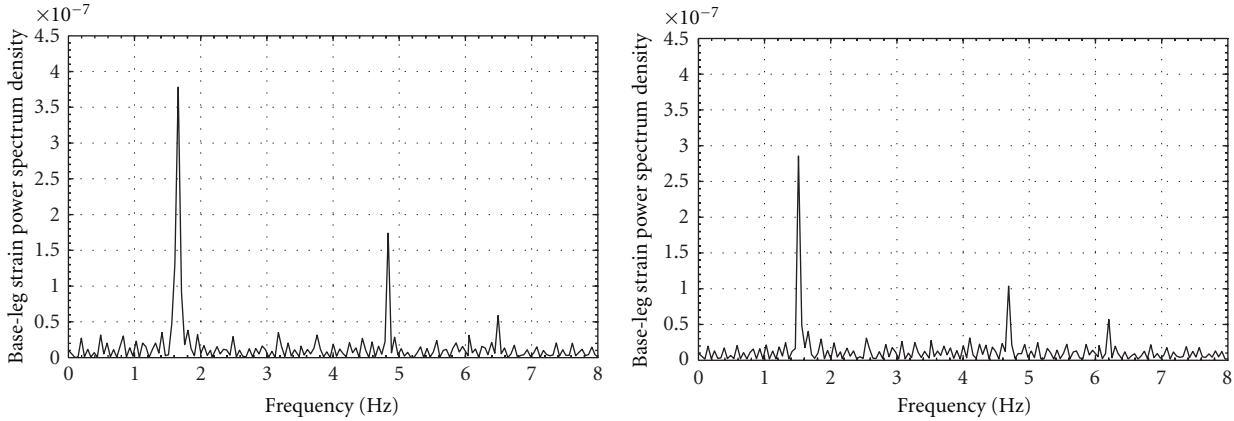

Figure 6: The power spectral density of strain at the base bottom: (a) without lines; (b) with lines.

main dynamic strain variation which reflected the bending moment GRF is similar to that of displacement dynamic response at the tower top, but the difference is that the bending moment GRF is larger than the displacement GRF, which may be caused by the larger displacement background component and instead of the relatively smaller strain background component.

4. Guasi-Static Method of GRF

4.1. Australian Load Code Method. The simplified Holmes GRF method for the lattice tower is applied in the Australian load code [15]. This approach assumes that only the first-order modal response of tower is considered and known the random load, such as the wind power spectrum density function. GRFs for the loading effect on the bending moment and shear are consistent and varying with altitudes. Usually, the wind loading duration is adopted from 10 min to 1 h. The GRF formula can be expressed as

$$G_s = 1 + rH\sqrt{g_B^2 B_s + g_R^2\left(\frac{SE}{\zeta}\right)}, \tag{5}$$

where $r = (2/M_t)(\sigma_V/\overline{V})$, $(\sigma_V/\overline{V})$ is the turbulence intensity on the tower height h, M_t means the terrain factor of mean wind velocity, H represents the factor for height, $H = 1 + 0.2(s/h)^2$, s denotes the height of the peak moment or shear, h stands for the transmission tower height above ground, and B_s represents the background factor, that is,

$$B_s = \left(1 + \sqrt{\frac{36(h-s)^2 + 64w_s^2}{L_h}}\right)^{-1}, \tag{6}$$

where w_s is the average structural width between h and s, $L_h = 1000(h/10)^{0.25}$, $g_B = g_u[1 + 0.925r\sqrt{B_s}]$, $g_u = 3.7$,

Table 6: GRF values calculated from various quasi-static methods.

No.	Mean wind velocity $\overline{V}_{56.9}$ (m/s)	Turbulence intensity	AD method (based on bending moment)	Holmes method (based on bending moment)	Holmes method (based on displacement)
1	8.70	0.06	2.278	2.269	2.238
2	9.48	0.75	2.747	2.700	2.650
3	10.36	0.10	3.348	3.204	3.130
4	11.44	0.11	4.373	4.378	4.241
5	12.09	0.13	4.471	4.521	4.366
6	13.21	0.14	4.692	4.762	4.591
7	14.21	0.16	4.559	4.618	4.456
8	15.03	0.15	3.279	3.246	3.172
9	13.65	0.13	3.150	3.116	3.051
10	11.90	0.11	2.907	2.861	2.804
11	9.36	0.09	2.662	2.608	2.562
12	7.45	0.08	2.434	2.382	2.347
Mean value			3.408	3.389	3.301

$g_R = \sqrt{2\ln(Tn)}$, T denotes the duration, usually taken to be 600 s, n means the nature frequency of the first order mode, and S is the scale factor for resonant response, that is,

$$S = \left\{\left[1 + \left(\frac{3.5nh}{\overline{V}_h}\right)\right]\left[1 + \left(\frac{4nw_0}{\overline{V}_h}\right)\right]\right\}^{-1}, \quad (7)$$

where w_0 means the average structural width between $h/2$ and h, $\overline{V}_h$ denotes the mean wind velocity on the calculation height h, and E represents the energy factor of gust, that is,

$$E = \frac{0.47N}{(2+N^2)^{5/6}}, \quad (8)$$

where $N = nL_h/\overline{V}_h$ is the conversion frequency and ζ means the limit damping ratio, for the bolted transmission tower, which is $\zeta = 0.05$.

On those conditions of various turbulence intensities and mean velocities of wind, the GRF based on the bending moment is calculated by means of the quasistatic method of Australian standard and the measurement data, and those results are shown in Table 4.

4.2. Holmes Quasistatic Method. The Holmes quasistatic method is a GRF one that is recommended by the Australian standard, which was proposed by Holmes in 1995 for the lattice tower design [16, 17]. This method can be used for calculating the GRFs based on the bending moment or shear which is varied with tower height and independent on the displacements at the tower top. The GRF at any height s of the tower is defined as the ratio of the peak value to the average, of which detailed formulas can be found in the literature [16].

(1) The Bending Moment Gust Factor. The bending moment GRF of the tower at any height is given by

$$G_m(s) = 1 + \frac{r\left[g_B^2 B_s F_7 + g_R^2 (SE/\zeta) F_3 F_4 F_8\right]^{1/2}}{F_6}, \quad (9)$$

where the denotations of r, g_B, g_u, g_R, S, and E have the same meanings with the Australian standard method.

$$B_s = 2\left[\frac{{}^zL_u}{(h-\mathrm{s})}\right] + 2\left[\frac{{}^zL_u}{(h-\mathrm{s})}\right]^2\left[e^{\{(s-h)/{}^zL_u\}} - 1\right],$$
$$ {}^zL_u = 25\left(\frac{h}{10}\right)^{0.25}, \quad (10)$$
$$\zeta = \zeta_s + \zeta_a,$$

where ζ_s means the structural damping, and ζ_a denotes the aerodynamic damping which can be expressed as

$$\zeta_a = \left[\frac{\rho C_d \delta \overline{V}_h h}{4\pi n_1 m_0}\right] F_9, \quad (11)$$

where ρ means the aerial density, C_d is the resistance coefficient, δ denotes the ratio of real area, $\overline{V}_h$ represents the mean velocity at tower top, m_0 means the mass per unit length at the tower top, and F_3, F_4, F_6, F_7, F_8, and F_9 are the simplified formula denotations, respectively, in which detailed expressions can be found in the literature [16].

(2) The Displacement GRF at the Tower Top. The displacement GRF at the tower top can be calculated by the following formula:

$$G_x = 1 + \frac{r\left[g_B^2 B_0 F_{11} + g_R^2 (SE/\zeta) F_3 F_4 F_{12}\right]^{1/2}}{F_{10}}, \quad (12)$$

where when $s = 0$, the expression of B_0 is fully same as B_s; also, F_3, F_4, F_{10}, F_{11}, and F_{12} are the simplified formula denotations, respectively, in which detailed expressions can be found in literature [16].

The GRFs based on the bending moment and displacements are shown in Table 6, which are calculated by the Holmes quasistatic method. From Table 6, it can be seen that

the GRF obtained from the Australian specification is consistent with the Holmes quasistatic method. It is not obvious to the analytical deviation for neither bending moment nor displacement as a computational input, in which the displacement GRF is slightly smaller, but the deviation between them is not more than 5%. In addition, compared with the aforementioned analytical results of measurement data, the bending moment GRF is approximately near to that of the quasistatic method, but the displacement GRF then marches in the opposite direction, which may be caused from the displacement background response.

5. Conclusions

Based on the field monitoring of transmission tower, in the parallel and orthogonal directions with the transmission line, respectively, the measurement data of fluctuating wind velocity with different turbulence intensities, various accelerations from the parts of tower, and dynamic strains of the main upright legs near the tower foundation are measured and collected. The dynamic characteristics and GRFs of the transmission tower are analyzed from the modal identification method, the FEM, and the quasistatic method, respectively. The results have been shown as follows.

(1) An approach based on multisensors on-site monitoring test, wind-induced vibration analyses, and quasistatic design for TTLS have been presented, which can provide a simplified method for TTLS design and vibration analyses.

(2) The dynamic characteristics of transmission tower determined by the modal identification approach with the measured data are consistent with those of the FEM, and the calculated deviation between them is about 5%, which shows that both analytical methods have the better compliance and validity.

(3) The GRFs from the measured data are very close to the bending moment GRFs analyzed by the two kinds of quasistatic methods, and those calculated values of the quasistatic method are slightly larger, but the deviations between them are within 5%.

(4) As for the displacement GRF, the calculated values from the measured data are less than those of quasistatic method, which may be caused by the larger background components of displacement response.

Acknowledgments

This research work is jointly supported by the Science Fund for Creative Research Groups of the National Natural Science Foundation of China (Grant no. 51121005), the National Natural Science Foundation of China (Grant nos. 51078051, 51178083, and 51222806), and the Program for New Century Excellent Talents in University of China (Grant no. NCET-10-0287).

References

[1] H. F. Lam and T. Yin, "Dynamic reduction-based structural damage detection of transmission towers: practical issues and experimental verification," *Engineering Structures*, vol. 33, no. 5, pp. 1459–1478, 2011.

[2] R. C. Battista, R. S. Rodrigues, and M. S. Pfeil, "Dynamic behavior and stability of transmission line towers under wind forces," *Journal of Wind Engineering and Industrial Aerodynamics*, vol. 91, no. 8, pp. 1051–1067, 2003.

[3] H. Li and H. Bai, "High-voltage transmission tower-line system subjected to disaster loads," *Progress in Natural Science*, vol. 16, no. 9, pp. 899–911, 2006.

[4] A. M. Loredo-Souza and A. G. Davenport, "A novel approach for wind tunnel modelling of transmission lines," *Journal of Wind Engineering and Industrial Aerodynamics*, vol. 89, no. 11-12, pp. 1017–1029, 2001.

[5] M. Takeuchi, J. Maeda, and N. Ishida, "Aerodynamic damping properties of two transmission towers estimated by combining several identification methods," *Journal of Wind Engineering and Industrial Aerodynamics*, vol. 98, no. 12, pp. 872–880, 2010.

[6] T. Yin, H. F. Lam, H. M. Chow, and H. P. Zhu, "Dynamic reduction-based structural damage detection of transmission tower utilizing ambient vibration data," *Engineering Structures*, vol. 31, no. 9, pp. 2009–2019, 2009.

[7] Y. Momomura, H. Marukawa, T. Okamura, E. Hongo, and T. Ohkuma, "Full-scale measurements of wind-induced vibration of a transmission line system in a mountainous area," *Journal of Wind Engineering and Industrial Aerodynamics*, vol. 72, no. 1–3, pp. 241–252, 1997.

[8] T. Okamura, T. Ohkuma, E. Hongo, and H. Okada, "Wind response analysis of a transmission tower in a mountainous area," *Journal of Wind Engineering and Industrial Aerodynamics*, vol. 91, no. 1-2, pp. 53–63, 2003.

[9] P. Harikrishna, J. Shanmugasundaram, S. Gomathinayagam, and N. Lakshmanan, "Analytical and experimental studies on the gust response of a 52 m tall steel lattice tower under wind loading," *Computers and Structures*, vol. 70, no. 2, pp. 149–160, 1999.

[10] E. Savory, G. A. R. Parke, M. Zeinoddini, N. Toy, and P. Disney, "Modelling of tornado and microburst-induced wind loading and failure of a lattice transmission tower," *Engineering Structures*, vol. 23, no. 4, pp. 365–375, 2001.

[11] M. J. Paluch, T. T. O. Cappellari, and J. D. Riera, "Experimental and numerical assessment of EPS wind action on long span transmission line conductors," *Journal of Wind Engineering and Industrial Aerodynamics*, vol. 95, no. 7, pp. 473–492, 2007.

[12] F.-Z. Fu and H.-X. Hua, *Mode Analytical Theory and Its Application*, Shanghai Jiaotong University, Shanghai, China, 2000.

[13] Y. Q. Ni, X. W. Ye, and J. M. Ko, "Modeling of stress spectrum using long-term monitoring data and finite mixture distributions," *Journal of Engineering Mechanics*, vol. 138, no. 2, pp. 175–183, 2012.

[14] Y. Q. Ni, X. W. Ye, and J. M. Ko, "Monitoring-based fatigue reliability assessment of steel bridges: analytical model and application," *Journal of Structural Engineering*, vol. 136, no. 12, pp. 1563–1573, 2010.

[15] AS 3995-1994, *Australian Standard for Design of Steel Lattice Towers and Masts*, Standards Australia, North Sydney, Australia.

[16] J. D. Holmes, "Along-wind response of lattice towers: part I—derivation of expressions for gust response factors," *Engineering Structures*, vol. 16, no. 4, pp. 287–292, 1994.

[17] J. D. Holmes, "Along-wind response of lattice towers—II. Aerodynamic damping and deflections," *Engineering Structures*, vol. 18, no. 7, pp. 483–488, 1996.